

## Long-lived transient anion of $c\text{-C}_4\text{F}_8\text{O}$

J. Kočišek,<sup>1</sup> R. Janečková,<sup>2</sup> and J. Fedor<sup>1</sup>

<sup>1</sup>*J. Heyrovský Institute of Physical Chemistry, Czech Academy of Sciences, Dolejškova 3, 18223 Prague, Czech Republic*

<sup>2</sup>*Department of Chemistry, University of Fribourg, Chemin du Musée 9, CH-1700 Fribourg, Switzerland*

We report partial cross sections for electron attachment to  $c\text{-C}_4\text{F}_8\text{O}$ , a gas with promising technological applications in free-electron-rich environments. The dissociative electron attachment leads to a number of anionic fragments resulting from complex bond-breaking and bond-forming processes. However, the anion with the highest abundance is the non-dissociated (transient) parent anion which is formed around 0.9 eV electron energy. Its lifetime reaches tens of microseconds. We discuss the origin of this long lifetime, the anion's strong interactions with other molecules, and the consequences for electron-scavenging properties of  $c\text{-C}_4\text{F}_8\text{O}$  in denser environments, in particular for its use in mixtures with  $\text{CO}_2$  and  $\text{N}_2$ .

### I. INTRODUCTION

Transient anions (resonances) formed in collisions of free electrons with molecules represent interesting species both from fundamental and from technological point of view. The fundamental interest stems from the fact that, once formed, they can lose the electron via its autodetachment. It usually happens on the time scale of femto- to picoseconds. This is comparable with typical time scales for motion of nuclei in molecules—both for vibrational or dissociative. The corresponding resonant cross sections thus reveal a number of ultrafast phenomena, often connected with the breakdown of Born-Oppenheimer approximation.<sup>1</sup> The technological interest stems from the fact that resonances act as intermediates in the electron-induced degradation of molecules and thus govern electron induced chemistry in a range of technological environments.

$c\text{-C}_4\text{F}_8\text{O}$ , perfluorotetrahydrofuran, is a gas which has been attracting increasing attention in recent years due to its promising technological applications. It performs well and environmentally friendly as a cleaning gas for chemical vapor deposition chambers,<sup>2</sup> and it is used as a novel radiative medium in Cherenkov detectors.<sup>3</sup> It has been also considered as a candidate for  $\text{SF}_6$  replacement in high voltage insulation.<sup>4</sup> The technological advantage of  $c\text{-C}_4\text{F}_8\text{O}$  is its high thermal stability<sup>5</sup> as well as compatibility with other materials.<sup>6</sup> In all these environments, interactions with free electrons play a crucial role which creates a need for detailed knowledge of the electron-driven chemistry of this compound.

Motivated by this need, we report partial cross sections for electron attachment to  $c\text{-C}_4\text{F}_8\text{O}$ . We have observed an unusual effect: a certain fraction of transient anions, created at energies considerably larger than thermal, has a lifetime longer than tens of microseconds. We unravel the origin of this rare phenomenon using density functional theory (DFT) calculations and discuss its implications for use of  $c\text{-C}_4\text{F}_8\text{O}$  in the above-mentioned technological environments.

### II. EXPERIMENT

The quantitative dissociative electron attachment (DEA) spectrometer has been described in detail previously.<sup>7–9</sup> The electron beam is produced by a trochoidal electron monochromator, passes through a collision cell filled with the sample gas, and is collected by a Faraday cup. Anions created by DEA are extracted through a narrow slit in the cell's wall to a time-of-flight (TOF) mass analyzer. The whole experiment is pulsed—the electron beam passes through the collision cell during 200 ns, while the cell is field-free, and after a delay (during which the electrons are allowed to leave the cell), a voltage pulse of  $-300$  V is applied across the cell to extract the anions. The delay between the electron pulse and the anion extraction is kept at 200 ns during cross-sectional measurements. For the sake of certain measurements (described in Sec. III), it has been stretched up to 25  $\mu\text{s}$ . The repetition frequency of the whole cycle is typically 50 kHz.

The TOF tube is constructed as a focusing ion lens, and the entire setup was designed to keep the extraction and detection efficiency independent of the mass and of the initial kinetic energy of the produced anions. The anions are detected by a microchannel plate coupled with a phosphor screen and a photomultiplier, counted and their arrival times are analyzed.

The pressure in the collision cell is controlled by a needle valve and monitored by a capacitance manometer. The cross sections are typically measured at  $(3\text{-}6) \times 10^{-4}$  Torr pressure range. The electron energy resolution is 250 meV, the electron current in the order of 10 nA in the CW mode, which drops to 0.1 nA in the pulsed mode. The electrons with energies down to 100 meV are present in the incident beam; this was verified by measuring the  $\text{SF}_6^-$  ion yield from  $\text{SF}_6$  which reaches very high values close to 0 eV.<sup>10</sup>

The electron energy scale and the absolute cross sections are calibrated using two compounds:  $\text{CO}_2$  and  $\text{HCOOH}$ . The production of  $\text{O}^-$  from  $\text{CO}_2$  has a vertical onset at 3.99 eV and the integrated cross section of 13.3  $\text{pm}^2 \text{eV}$ .<sup>11</sup> The production

of  $\text{HCOO}^-$  from  $\text{HCOOH}$  has an onset at 1.29 eV and the integrated cross section of  $156 \text{ pm}^2 \text{ eV}$ .<sup>12</sup> The two independent calibrations were in excellent agreement. The error of the absolute measurements (two standard deviations) is taken to be  $\pm 20\%$ .

### III. RESULTS AND DISCUSSION

#### A. Partial electron attachment cross sections

Figures 1 and 2 show partial cross sections for all negative ions that were detected following the low-energy electron impact on  $c\text{-C}_4\text{F}_8\text{O}$ . The panels are ordered according to the decreasing cross section. In the present case, the chemical formulas of produced anions are unambiguously determined by the fragment masses. The fragments are produced solely in the energy range 0–6.5 eV. No signals were observed at higher electron energies up to the onsets of non-resonant ion-pair formation. This is in strong contrast with tetrahydrofuran (THF)  $c\text{-C}_4\text{H}_8\text{O}$  which has a number of dissociative electron attachment peaks in the energy region between 6 and 12 eV and no detectable signals at lower energies.<sup>13</sup> The most probable reason for this strong difference is the energetics. The threshold energies for DEA channels in THF will be higher due to the lower electron affinity of hydrogen compared to fluorine. Many of the low-energy resonances may thus be below the dissociation threshold. Even though, from the same reason, the shape resonances in THF will lie at higher energies, and this is often connected with larger width toward autodetachment, hence causing a negligible DEA cross section.

The signal appears at four resonances with peak positions of 0.9, 1.6, 2.5, and 4.0 eV. The large number of fragment anions that must have very different structures points out to

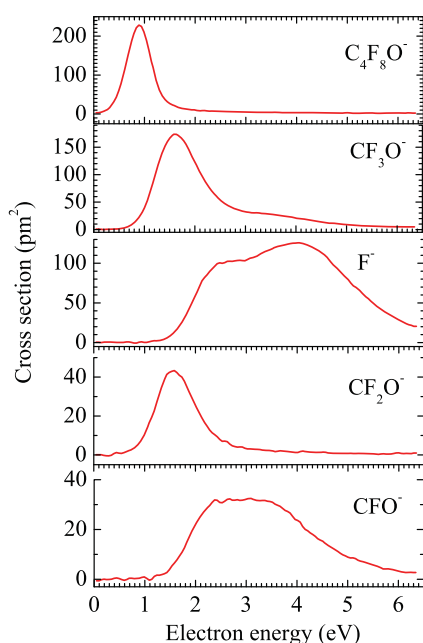


FIG. 1. Partial cross sections for the production of the first group of anions following the electron attachment to  $c\text{-C}_4\text{F}_8\text{O}$ . As discussed in the text, the measured cross section for the parent anion  $\text{C}_4\text{F}_8\text{O}^-$  will depend on its detection time, and the present data correspond to a detection time of  $7.6 \mu\text{s}$ .

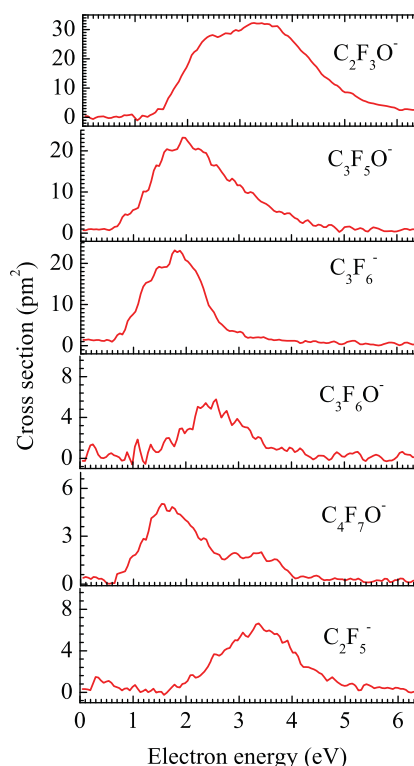


FIG. 2. Partial cross sections for the production of the second group of anions following the electron attachment to  $c\text{-C}_4\text{F}_8\text{O}$ .

numerous dissociative pathways with complex bond-breaking and bond-forming reaction steps. Such complex scrambling of constituent atoms is one of the characteristic features of molecular decomposition via resonant electron attachment, and it has been observed for a number of organic target molecules.<sup>14,15</sup>

The most striking observation is the presence of the parent anion  $\text{C}_4\text{F}_8\text{O}^-$ . Its detection time in the standard experimental configuration for cross-sectional measurements (200 ns delay between the electron and the extraction pulse) is  $7.6 \mu\text{s}$  after its formation. As discussed below, the survival of the parent anion to such a long time scale is a rare phenomenon, observed only in a small number of molecules. In order to be certain that the transient anion is not stabilized by collisions with other molecules in the collision chamber, the pressure dependence of the  $\text{C}_4\text{F}_8\text{O}^-$  signal is shown in Fig. 3. Two fragment ions,  $\text{CF}_3\text{O}^-$  and  $\text{CF}_2\text{O}^-$ , are shown for comparison. The pressure dependence is clearly linear. The survival up to the experimental observation time window is thus a property of the isolated transient anions.

The abundance of the parent anion will be a function of this observation time window due to excess of internal energy. We have attempted to observe the eventual decrease of the  $\text{C}_4\text{F}_8\text{O}^-$  signal due to its decay by varying the delay between the electron pulse passing the collision chamber and the anion extraction pulse. The observation time window was varied between 7 and  $30 \mu\text{s}$ . We observed a certain decrease of the signal with the delay; however, the signal of all fragment anions decreased by the same amount. The same holds for the decrease of the signal of the calibration anions  $\text{O}^-/\text{CO}_2$  and  $\text{HCOO}^-/\text{HCOOH}$ . This is caused by the initial velocity

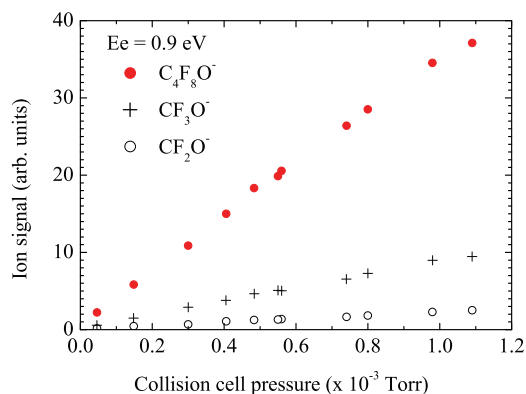


FIG. 3. Pressure dependence of the signal intensity for parent and two fragment anions.

of neutral molecules from their Maxwell-Boltzmann velocity distribution: during the longer delay between the electron pulse and repeller pulse, the anions leave the active extraction region of the collision chamber. The delay experiments were thus inconclusive for the lifetime determination. Experiments on a dedicated instrument, e.g., a storage ring, would be necessary to resolve the question of the natural parent anion lifetime.

### B. Origin of the long parent anion lifetime

The observed parent anion is necessarily metastable: the electron energy plus the electron affinity is stored within the internal degrees of freedom, and (at single collision conditions) the anion will decay either by electron detachment or fragmentation. Survival of the transient anions up to microseconds has been reported only for a small number of molecular targets. They can be basically divided into two groups: (i) those formed at thermal energies (close to 0 eV) and (ii) those formed at higher electron energies. In the group (i), the detection probability is considerably enhanced by extremely large attachment cross sections, often reaching the  $\pi\lambda^2$  limit of the s-wave reactive capture cross section (given by the de Broglie wavelength of the incident electron). This behavior occurs, for example, in a range of halogenated hydrocarbons.<sup>16</sup> The typical example is SF<sub>6</sub>, for which its peculiar properties and wide usage lead to the fact that it is perhaps the most studied electron attachment target.<sup>17</sup> The group (ii), where the electron capture cross section has generally much lower values, is much smaller. Long-lived transient anions to our knowledge were detected for *p*-benzoquinone at 2.1 eV,<sup>18</sup> tetrafluoro-*p*-benzoquinone at 0.5 eV,<sup>19</sup> azulene at 0.35 eV,<sup>20</sup> nickelocene at 1 eV,<sup>21</sup> chlorodifluoroacetic acid at 0.75 eV,<sup>22</sup> and duroquinone at 1.8 eV.<sup>23</sup> For the majority of these molecules, the detailed stabilization—or better to say, metastability—mechanisms are not known.

The present transient anions are formed at 0.9 eV. The theoretical description of the involved resonant electronic state would require full scattering calculations which are beyond the scope of the present work. In any case, it is not a critical point: the C<sub>4</sub>F<sub>8</sub>O<sup>-</sup> anions that are detected are certainly not in a resonant electronic state. It is highly improbable that a resonant state has a microsecond lifetime towards the electron detachment. Rather, upon the (vertical) electron attachment,

the molecular geometry will rapidly change such that an electronically bound anion is formed which becomes vibrationally highly excited via intramolecular vibrational redistribution (IVR). The total energy is still in the continuum, randomized over the vibrational modes of C<sub>4</sub>F<sub>8</sub>O<sup>-</sup>.

Using the B3LYP functional together with the 6-31+G(2df) basis set, we have identified the mechanism of this process. This method and basis set have been previously shown to provide a reliable description of the bound anions, both of the asymptotic energies and of the qualitative potential energy surfaces.<sup>14,15</sup> The lowest-energy geometry of the neutral *c*-C<sub>4</sub>F<sub>8</sub>O molecule is that with the C<sub>2</sub> symmetry, shown in Fig. 4, lower left panel. Figure 4 also shows the optimized structure of the electronically bound C<sub>4</sub>F<sub>8</sub>O<sup>-</sup> anion that is closest to the geometry of the neutral molecule. As can be seen, the molecular frame structures of the neutral and bound anion are similar with one crucial exception: the carbon–fluorine bond on the carbon atom that is further away from the oxygen is prolonged from 1.3 Å in the neutral to 2.0 Å in the anion. The extra electron in the anion is localized mostly on the distant fluorine atom: the Mulliken charge on this atom is −0.61 e. Correspondingly, this anionic structure has a rather large dipole moment of 4.7 D.

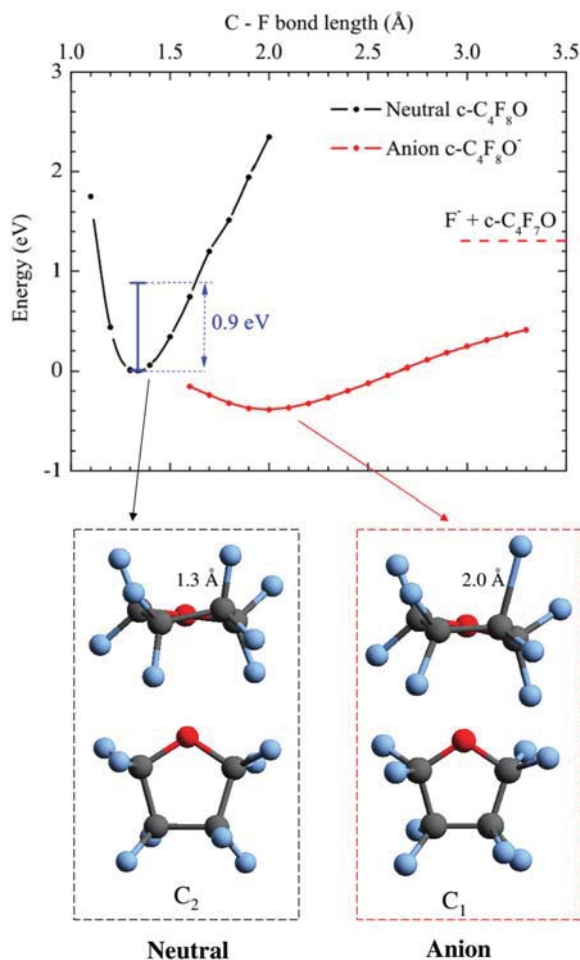


FIG. 4. (Top) Relaxed potential energy scans along the C–F bond on the carbon atom further from the oxygen, both for the neutral and electronically bound anion of *c*-C<sub>4</sub>F<sub>8</sub>O. (Bottom) Optimized structures of the neutral (left) and anion (right).

The top panel of Fig. 4 shows relaxed potential energy scans along the decisive C–F bond. The black line corresponds to the neutral molecule, the red line corresponds to the cyclic anion. For the sake of graphical simplicity, zero-point energies are not considered (when all vibrations are considered, zero-point energy of the neutral is 1.42 eV). At the bond lengths shorter than the (not shown) crossing point between the anion and neutral curves, the quantum chemical methods cannot be used to describe the anion since the additional electron in the continuum would be bound only by the finite size of the basis set. Nonetheless, it is reasonable to assume that the continuum electronic state which is formed around 0.9 eV electron energy (shown as the vertical bar) correlates with the calculated bound anion state. The continuum (resonant) state is repulsive, and upon its formation, the C–F bond prolongs which may happen very fast, presumably on the picosecond time scale. Beyond the crossing point, the anion becomes electronically bound and the electron detachment channel is closed. The bond can of course contract again for the autodetachment channel to open. However, IVR is known to be an ultrafast process<sup>24</sup> and the excess energy is randomized over the vibrational modes of  $\text{C}_4\text{F}_8\text{O}^-$ . In the present case, the excess energy is 1.4 eV (the calculated adiabatic electron affinity of *c*- $\text{C}_4\text{F}_8\text{O}$  is 0.5 eV). Because of the high masses of the constituent atoms, the vibrational modes have small spacing and consequently the anion has high vibrational density of states. This causes a long time required for the system to return to a configuration which will lead either to autodetachment or to fragmentation. Apparently, for a certain fraction of anions, this time even exceeds 30  $\mu\text{s}$  which is the longest observation window of the present experiment.

### C. Consequences for attachment properties in denser environments

We have recently reported<sup>25</sup> electron transport properties of *c*- $\text{C}_4\text{F}_8\text{O}$  measured in diluted mixtures with the buffer gases  $\text{N}_2$ ,  $\text{CO}_2$ , and Ar. These experiments were performed at total pressures of 20–100 mbar and at the *c*- $\text{C}_4\text{F}_8\text{O}$  concentration of 0.5%. The experimental observations can be summarized into two points: (i) the effective electron attachment rates are unusually strongly dependent on the pressure of the mixture and (ii) this dependence is much stronger in mixtures of  $\text{CO}_2$  than that in mixtures with  $\text{N}_2$ . These observations were interpreted by a strong role of three-body attachment, and this was quantitatively described in terms of various rate coefficients. The present results elucidate the molecular mechanism of this effect.

The three-body attachment is caused by a collisional stabilization of the transient anion with the buffer gas molecules *M*.



The asterisk denotes the transient anion, and its excess energy is carried away by the collision partner. In order to be operative, the mean time between collisions has to be shorter than the lifetime of the transient anion. The mean time between *c*- $\text{C}_4\text{F}_8\text{O}^{-*} + \text{M}$  collisions can be determined from the estimate of the collisional diameter.<sup>26</sup> The main component in the long-range intermolecular interaction between the anion and a nonpolar collision partner *M* is the ion induced dipole

interaction with the potential

$$V(r) = -\frac{1}{4\pi\epsilon_0} \frac{\alpha e^2}{r^4}, \quad (2)$$

where  $\alpha$  is the polarizability volume of *M* and  $e$  is the elementary charge. In order to quantify the effectiveness of the collisional stabilization we use a capture cross section where two collision partners for a short-lived complex. Of course, the formation of such a complex does not ensure that the collision leads to anion stabilization. On the other hand, the anion can be stabilized also in other inelastic collisions that do not form such a complex, so we use  $\sigma_{\text{capt}}$  as a suitable representation for the order of magnitude.

For a central potential of the form  $V(r) = -a/r^4$ , the classical capture cross section is  $\sigma_{\text{capt}} = \pi \sqrt{8 \frac{a}{\mu v^2}}$  (e.g., Ref. 27), where  $\mu$  is the reduced mass of the collision partners and  $v$  is their relative velocity. Using potential (2) and the mean relative velocity of an ideal gas  $v = \sqrt{\frac{8kT}{\pi\mu}}$ , one arrives at the following estimate of the capture cross section:

$$\sigma_{\text{capt}} = \pi \sqrt{\frac{e^2 \alpha}{4\epsilon_0 kT}}. \quad (3)$$

This expression, with substituted molecular parameters for  $\text{CO}_2$ , leads to a capture cross section of 207.8  $\text{\AA}^2$  and a corresponding collisional diameter of 8.1  $\text{\AA}$ . This gives a mean time between  $\text{C}_4\text{F}_8\text{O}^{-*} + \text{M}$  collisions 2.4 ns at 20 mbar pressure and 0.5 ns at 100 mbar pressure.

A considerable fraction of transient anions can be thus collisionally stabilized in the denser environment, which are not detected in a single-collision-condition experiment (such as the present one) due to autodetachment. This explains why the attachment rates calculated from the beam data are much lower than the ones measured in the mixtures,<sup>25</sup> and it gives rise to the strong pressure dependence observed in the latter.

The observed difference between the two buffer gases suggests that the collisional stabilization is more effective when *c*- $\text{C}_4\text{F}_8\text{O}$  is mixed with  $\text{CO}_2$  than when mixed with  $\text{N}_2$ . This means that the cross section for the *c*- $\text{C}_4\text{F}_8\text{O}^- + \text{CO}_2$  collision has to be larger than the cross section for the *c*- $\text{C}_4\text{F}_8\text{O}^- + \text{N}_2$  collision. The polarizability volume of  $\text{N}_2$  (1.7  $\text{\AA}^3$ ) is smaller than that of  $\text{CO}_2$  (2.6  $\text{\AA}^3$ ), which goes in line with this finding. To validate it further, we have probed the interaction between the cyclic structure of the bound anion with both collision partners. For this purpose, we have used the B3LYP-D3 method that includes empirical dispersion correction<sup>28</sup> with the 6-31+G(d) basis set. We have identified numerous local minima of the *c*- $\text{C}_4\text{F}_8\text{O}^- \cdot \text{M}$  (*M* =  $\text{CO}_2$  or  $\text{N}_2$ ) complex, and the bottom panel of Fig. 5 shows the ones with the lowest energies. We have also performed relaxed potential energy scans along the pathways shown in Fig. 5. The curves illustrate a large difference in the mutual interaction: the binding energy of the *c*- $\text{C}_4\text{F}_8\text{O}^- \cdot \text{CO}_2$  complex is 0.37 eV, while that of the *c*- $\text{C}_4\text{F}_8\text{O}^- \cdot \text{N}_2$  complex is 0.11 eV. It should be noted that the numerous structures of these complexes are rather close in energy and the choice of the lowest-energy will depend on the used computational method, but this is not a crucial factor for present conclusions. The relation between the binding

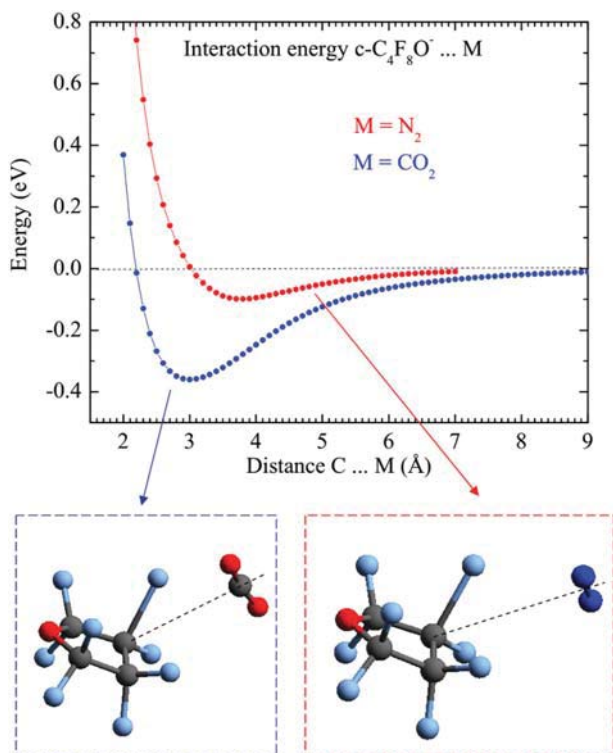


FIG. 5. Relaxed potential energy scans between the  $c\text{-C}_4\text{F}_8\text{O}^-$  anion and the collision partners  $\text{CO}_2$  and  $\text{N}_2$  along the indicated lines. The  $\text{C}\cdots\text{M}$  distance corresponds to the carbon atom indicated by these lines.

energy of the collision complex and the collisional cross section between the transient anion and the buffer gas partner is of course not straightforward. Also, the effectivity of the collisional stabilization will depend on other factors, e.g., the energy transfer rate between the partners. Nonetheless, due to the difference of more than a factor of three in the mutual interaction energies, it is reasonable to assume that the different pressure dependence of attachment rates in these gases can be attributed to a different rate of collisional stabilization of transient anions.

#### IV. CONCLUSIONS

In conclusion, we have measured partial cross sections for electron attachment to  $c\text{-C}_4\text{F}_8\text{O}$  at single-collision conditions. Apart from a number of fragment ions resulting from the dissociative electron attachment, we have also observed the transient anion  $c\text{-C}_4\text{F}_8\text{O}^-$  with a lifetime exceeding tens of microseconds. DFT calculations revealed that the most probable stabilization mechanism of this transient anion is that upon electron attachment one of the C–F bonds rapidly stretches, which closes the vertical autodetachment channel. The IVR then leads to vibrationally hot anion, which due to the high vibrational heat capacity stores the energy for the time scales that correspond to the observation time window of our experiment. The long-liveness of the parent anion and the fact that its abundance will naturally decrease with time have profound consequences for electron attachment properties of this gas. If it is used at moderate pressures, the collisions with neighbouring molecules stabilize the transient anions. The electrons that at single-collision conditions autodetach thus

remain attached to the molecule in the form of stable anions. The apparent attachment cross section then strongly depends on the environment: it does not only increase with pressure but depends also on the type of collision partners (buffer gas) since the effectiveness of the collisional stabilization depends on the interaction of the anion with the buffer gas molecules. We have shown that for the  $\text{CO}_2$  and  $\text{N}_2$  buffer gases, the collision-complex energy is different by more than a factor of three.

The present observations point out to several issues. The first is perhaps slightly discouraging: an ever-present motivation for measuring electron-collision cross sections is that they can be used as input in the models describing the free-electron-rich environments, e.g., plasmas. In the case of the present target (and range of others with metastable transient anions), the single-collision cross sections completely fail to describe electron transport properties even at moderate pressures (20–100 mbar). An educated scaling of the cross section (for example, as a part of a swarm normalization procedure<sup>29,30</sup>) is necessary, both at various pressures and in various buffer gases in order to account for the various stabilization rates of the long-lived transient anions.

The second issue concerns the potential applications. Considering that  $c\text{-C}_4\text{F}_8\text{O}$  has been considered as an alternative high-voltage insulation gas, the present cross sections are remarkably low. They peak around  $250 \text{ pm}^2$ , and the total energy-integrated cross section is  $1150 \text{ pm}^2 \text{ eV}$ . For comparison, the energy-integrated attachment cross sections in  $\text{SF}_6$  reach  $3 \times 10^5 \text{ eV pm}^2$ .<sup>10,17</sup> However, the high-voltage electric switch gears are often filled with 5–7 bars of the insulating gas or mixture. At such high pressures, the mean time between collisions of the transient anion with other gas molecules is in the order of 10 ps. This may lead to an increase of the attachment cross section by several orders of magnitude and thus considerably improve the dielectric strength of the gas.

#### ACKNOWLEDGMENTS

The authors thank Professor C. M. Franck and his group, ETH Zurich, for generous sample of  $c\text{-C}_4\text{F}_8\text{O}$  and for fruitful discussions. This work was supported by the Project No. 17-04844S of the Czech Science Foundation.

- <sup>1</sup>I. I. Fabrikant, S. Eden, N. J. Mason, and J. Fedor, *Adv. At., Mol., Opt. Phys.* **66**, 545 (2017).
- <sup>2</sup>K. J. Kim, C. H. Oh, N. E. Lee, J. H. Kim, J. W. Bae, G. Y. Yeom, and S. S. Yoon, *J. Vac. Sci. Technol., B: Microelectron. Nanometer Struct.* **22**, 483 (2004).
- <sup>3</sup>T. V. Acconcia *et al.*, *Nucl. Instrum. Methods Phys. Res., Sect. A* **767**, 50 (2014).
- <sup>4</sup>M. Rabie and C. M. Franck, *IEEE Trans. Dielectr. Electr. Insul.* **22**, 296 (2015).
- <sup>5</sup>C. J. Cobos, K. Hintzer, L. Solter, E. Tellbach, A. Thalerb, and J. Troe, *Phys. Chem. Chem. Phys.* **19**, 3159 (2017).
- <sup>6</sup>L. Pruette, S. Karecki, R. Reif, L. Tousingant, S. K. W. Reagen, and L. Zazzera, in *Environmental Issues in the Electronics and Semiconductor Industries*, edited by L. Mendicino and L. Simpson (Pennington, 1999), p. 20.
- <sup>7</sup>J. Fedor, O. May, and M. Allan, *Phys. Rev. A* **78**, 032701 (2008).
- <sup>8</sup>O. May, J. Fedor, and M. Allan, *Phys. Rev. A* **80**, 012706 (2009).
- <sup>9</sup>K. Graupner, S. A. Haughey, T. A. Field, C. A. Mayhew, T. H. Hoffmann, O. May, J. Fedor, M. Allan, I. I. Fabrikant, E. Illenberger *et al.*, *J. Phys. Chem. A* **114**, 1474 (2010).

- <sup>10</sup>M. Braun, S. Marienfeld, M. W. Ruf, and H. Hotop, *J. Phys. B: At. Mol. Phys.* **42**, 125202 (2009).
- <sup>11</sup>O. May, J. Fedor, B. C. Ibănescu, and M. Allan, *Phys. Rev. A* **77**, 040701(R) (2008).
- <sup>12</sup>R. Janečková, D. Kubala, O. May, J. Fedor, and M. Allan, *Phys. Rev. Lett.* **111**, 213201 (2013).
- <sup>13</sup>R. Janečková, O. May, A. R. Milosavljević, and J. Fedor, *Int. J. Mass Spectrom.* **365-366**, 163 (2014).
- <sup>14</sup>B. C. Ibanescu, O. May, A. Monney, and M. Allan, *Phys. Chem. Chem. Phys.* **9**, 3163 (2007).
- <sup>15</sup>R. Janečková, O. May, and J. Fedor, *Phys. Rev. A* **86**, 052702 (2012).
- <sup>16</sup>R. N. Compton, L. G. Christophorou, G. S. Hurst, and P. W. Reinhardt, *J. Chem. Phys.* **45**, 4634 (1966).
- <sup>17</sup>J. Troe, T. M. Miller, and A. A. Viggiano, *J. Chem. Phys.* **127**, 244303 (2007).
- <sup>18</sup>M. Allan, *Chem. Phys.* **81**, 235 (1983).
- <sup>19</sup>C. D. Cooper, W. F. Frey, and R. N. Compton, *J. Chem. Phys.* **69**, 2367 (1978).
- <sup>20</sup>L. G. Christophorou, *Adv. Electron. Electron Phys.* **46**, 55 (1978).
- <sup>21</sup>G. M. Begun and R. N. Compton, *J. Chem. Phys.* **58**, 2271 (1973).
- <sup>22</sup>J. Kopyra, C. König-Lehmann, I. Szamrej, and E. Illenberger, *Int. J. Mass Spectrom.* **285**, 131 (2009).
- <sup>23</sup>O. G. Khvosteno, V. G. Lukin, and E. E. Tseplin, *Rapid Commun. Mass Spectrom.* **26**, 2535 (2012).
- <sup>24</sup>R. Marquardt and M. Quack, in *Handbook of High Resolution Spectroscopy*, edited by M. Quack and F. Merckt (Wiley, 2011), Vol. 1, p. 511.
- <sup>25</sup>A. Chachereau, J. Fedor, R. Janečková, J. Kočišek, M. Rabie, and C. M. Franck, *J. Phys. D: Appl. Phys.* **49**, 375201 (2016).
- <sup>26</sup>M. Zawadzki, M. Ranković, J. Kočišek, and J. Fedor, "Dissociative electron attachment and anion-induced dimerization in pyruvic acid," *Phys. Chem. Chem. Phys.* (published online).
- <sup>27</sup>L. D. Landau and E. M. Lifshitz, *Mechanics* (Butterworth-Heinemann, 1981).
- <sup>28</sup>S. Grimme, J. Antony, S. Ehrlich, and H. Krieg, *J. Chem. Phys.* **132**, 154104 (2010).
- <sup>29</sup>Z. L. Petrovic, M. Suvakov, Z. Nikitovic, S. Dujko, O. Sasic, J. Jovanovic, G. Malovic, and V. Stojanovic, *Plasma Sources Sci. Technol.* **16**, S1 (2007).
- <sup>30</sup>J. Miric, D. Bosnjakovic, I. Simonovic, Z. Petrovic, and S. Dujko, *Plasma Sources Sci. Technol.* **25**, 065010 (2016).